Ab Initio Study of Intramolecular Ring Cyclization of Protonated and BF_3-Coordinated *trans*- and *cis*-4,5-Epoxyhexan-1-ol

James M. Coxon* and Aaron J. Thorpe

Department of Chemistry, University of Canterbury, Christchurch, New Zealand

Received March 1, 1999

The potential energy surface for the rearrangement of *cis*- and *trans*-4,5-epoxyhexan-1-ol with acid and the Lewis acid BF_3 to five- and six-membered cyclic ethers has been investigated by ab initio methods. The transition structures involving both inversion and retention of configuration at the reaction center at the HF/6-31G* and B3LYP/6-31G* levels are characterized. The preference for furan formation over pyran is attributed to the more favorable O−C_{ep}−O bond angles at the transition structures for furan formation. The torsional O−C_{ep}−C_{ep}−O angles associated with tetrahydrofuran and tetrahydropyran formation vary with structure and do not directly correlate with the preferred pathway.

Introduction

Ring opening of epoxides with a proton or Lewis acid is an important method in chemical synthesis of initiating intramolecular ring closure. Catalytic antibodies (e.g., 26D9) elicited to an antigen, *N*-[2-arylethyl]piperidine-*N*-oxide, have been developed by Janda and Lerner[1] to effect rearrangement of *trans*-8-aryl-4,5-epoxyheptan-1-ols enantioselectively to 6-*endo*-*tet*-tetrahydropyrans,[2−4] rather than to the chemically favored tetrahydrofurans (Figure 1). The catalytic antibodies effect chiral selection and overcome the stereoelectronic preference for five- over six-membered ring formation.

The reaction in the presence of the catalytic antibody is considered to arise because the transition structure to the tetrahydropyran has similarities to the hapten. The catalytic effect reflects an interplay between electronic stabilization (the hapten carrying a positive nitrogen) and general acid−base catalysis. Houk has carried out single point MP2/6-31G* calculations on the HF/6-31G* optimized geometries for the transition structure of a model system, *trans*-4,5-epoxyhexan-1-ol, lacking the aryl group and estimated[5] that the catalytic antibody must lower the 6-*endo* activation energy 3.6 kcal/mol more than it lowers the five-*exo* activation barrier. Calculations have been used to show the effect of a proximate acid source and counterion in influencing transition state structure, thereby mimicking the regiochemistry dictated by the catalytic antibody.[6] However, a complex[7] of the five-membered transition structure with the Houk theozyme 3.5 kcal/mol lower in energy than the complex previously

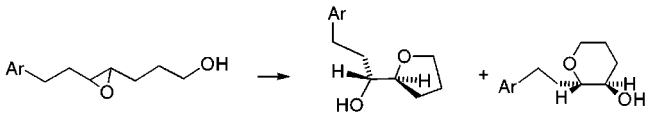

Figure 1. Intramolecular rearrangement of *trans*-7-aryl-4,5-epoxyheptan-1-ol to 5-*exo*-*tet* and 6-*endo*-*tet* products.

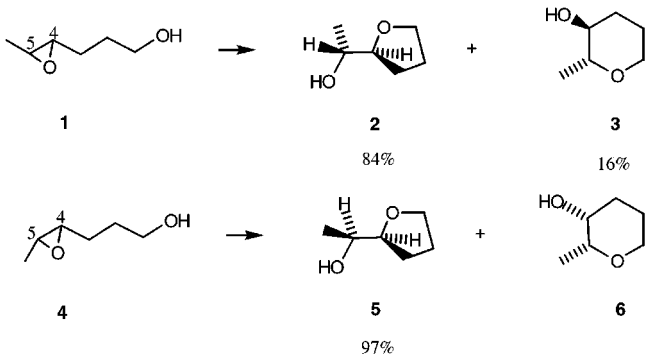

Figure 2. BF_3-catalyzed rearrangement of *cis*- and *trans*-4,5-epoxyhexan-1-ol.

reported[6] as a model for the antibody reverses the preference of that theozyme to favor furan formation, negating the theozyme as a model for the antibody reaction.[7]

We have previously reported the rearrangement of *trans*-4,5-epoxyhexan-1-ol (**1**) with BF_3−Et_2O to give *trans*-(1*RS*,2′*RS*)-1-(tetrahydrofuran-2′-yl)ethanol (**2**) (84%) and tetrahydropyran **3** (16%) (Figure 2). Under the same conditions, *cis*-4,5-epoxyhexan-1-ol (**4**) rearranges to give *cis*-(1*SR*,2′*RS*)-1-(tetrahydrofuran-2′-yl)ethanol (**5**) (97%).[8] The stereochemistry of the products is the result of intramolecular nucleophilic attack of the hydroxy oxygen at either C4 or C5 with inversion of configuration.

The preferential formation of the furan products **2** and **5** from **1** and **4** (*5-exo-tet* process) over the pyran products

(1) Janda, K. D.; Shevlin, C. G.; Lerner, R. A. *Science* **1993**, *259*, 490.

(2) Na, J.; Houk, K. N.; Shevlin, C. G.; Janda, K. D.; Lerner, R. A. *J. Am. Chem. Soc.* **1993**, *115*, 8453.

(3) Janda, K. D.; Shelvin, C. G.; Lerner, R. A. *Science* **1993**, *259*, 490−493. Janda, K. D.; Shelvin, C. G.; Lerner, R. A. *J. Am. Chem. Soc.* **1995**, *117*, 2659−2660.

(4) No tetrahydrofuran could be detected in the product.

(5) In the absence of the catalytic antibody, the five-*exo* process is calculated to be favored by 1.8 kcal/mol (single point solvent calculation, HF/6-31G* (SCRF)).[2] Assuming a negligible entropic difference in the two transition structures, this translates to a 96:4 product ratio at 25 °C. "To favor the 6-*endo* product to a similar amount, the catalytic antibody must lower the 6-*endo* activation energy 3.6 kcal/mol more than it lowers the 5-*exo* activation barrier."[2]

(6) Na, J.; Houk, K. N. *J. Am. Chem. Soc.* **1996**, *118*, 9204.

(7) An alternative theozyme has been determined that favors pyran formation over furan formation consistent with the antibody result. Thorpe, A. PhD Thesis, University of Canterbury, 1999. Coxon, J. M.; Thorpe, A. J., submitted for publication.

(8) Coxon, J. M.; Hartshorn, M. P.; Swallow, W. H. *Aust. J. Chem.* **1973**, *26*, 2521.

10.1021/jo990364d CCC: $18.00
Published on Web 07/02/1999

Table 1. Energies of Transition Structures

transition structures	optimization	energy (au)	ZPVE (au)	energy + scaled ZPVE (au)[b]	imag freq
		H^+			
TS **8** (inv) 5TS *trans*	HF/6-31G*	−384.208 82	0.201 65	−384.028 75	266
TS **9** (inv) 6TS *trans*	HF/6-31G*	−384.207 39	0.201 42	−384.027 52	255
TS **13** (inv) 5TS *trans*	HF/6-31G*	−384.208 53	0.202 02	−384.028 13	259
		−386.598 07[a]			
TS **14** (inv) 6TS *trans*	HF/6-31G*	−384.207 86	0.201 56	−384.027 87	261
	B3LYP/6-31G*	−386.600 09	0.188 17	−386.419 26	246
		−386.595 97[a]			
TS **18** (inv) 5TS *cis*	HF/6-31G*	−384.206 13	0.202 33	−384.025 45	255
		−386.595 44[a]			
TS **19** (inv) 6TS *cis*	HF/6-31G*	−384.203 84	0.201 55	−384.023 86	298
	B3LYP/6-31G*	−386.595 99	0.188 21	−386.415 12	282
		−386.591 87[a]			
TS **20** (ret) 5TS *cis*	HF/6-31G*	−384.193 34	0.200 88	−384.013 96	219
TS **21** (ret) 6TS *cis*	HF/6-31G*	−384.177 92	0.200 44	−383.998 93	171
	B3LYP/6-31G*	−386.569 60	0.186 70	−386.389 90	216
		BF_3			
TS **24** (inv) 5TS *trans*	HF/6-31G*	−707.044 66	0.205 69	−706.860 98	306
		−710.799 41[a]			
TS **25** (inv) 6TS *trans*	HF/6-31G*	−707.044 23	0.204 76	−706.861 38	309
		−710.797 30[a]			
TS **29** (inv) 5TS *cis*	HF/6-31G*	−707.045 49	0.205 15	−706.862 3	296
		−710.800 07[a]			
TS **30** (inv) 6TS *cis*	HF/6-31G*	−707.046 38	0.205 01	−706.863 31	302
		−710.801 92[a]			
TS **32** (inv) 5TS *trans*	HF/6-31G*	−707.042 67	0.205 45	−706.859 2	307
		−710.797 83[a]			
TS **33** (inv) 6TS *trans*	HF/6-31G*	−707.047 46	0.204 72	−706.864 65	262
	B3LYP/6-31G*	−710.806 08			
		−710.801 44[a]			

[a] B3LYP/6-31G* single point calculation on HF/6-31G* optimized structures. [b] ZPVE scaled by 0.961 (B3LYP) and 0.893 (HF).

3 and **6** (*6-endo-tet* process) is thought[8] to reflect a more favorable trajectory of the S_N2 attack of the hydroxy oxygen to C4 and concomitant reduction in transition structure ring strain. The present study seeks to define these parameters along with the bond and torsional angles associated with the transition structures. Baldwin[9] defined rules for ring closure, based on the perceived stereochemical requirements of the transition states leading to ring formation. What is of particular interest in the present study is that the departing nucleophile, as well as the incoming nucleophile, are both connected to the system and the transition structures are bicyclic (Figure 3).

The optimum values of the O−C_{ep}−O angle (α) (154.9°) and O−C_{ep}−C_{ep}−O torsional angle (177.1°) for nucleophilic attack at the protonated epoxide (Figure 3) follow from a computational study[10] of the reaction of water with protonated ethylene oxide. These values reflect frontier orbital overlap of the HOMO of the nucleophile and the LUMO of protonated ethylene oxide.[11] We have previously reported ab initio calculations on the acid-catalyzed rearrangement of *cis*- and *trans*-3,4-epoxypentan-1-ol.[12] The calculations were in agreement with the experimental results showing furan formation to be favored in preference to oxetane via five- and four-membered transition structures, respectively. The lower energy five-membered transition structures were found to be earlier and substantially looser than the four-membered transition structures. The O−C_{ep}−C_{ep}−O torsional angles in the five-membered transition structures, which are in the range 155−161°, show that optimum antiperiplanar orbital overlap at the reaction center was not achieved. The transition structures reflect a compromise between conformational ring strain and attainment of an optimum trajectory angle and antiperiplanar O−C_{ep}−C_{ep}−O transition geometry. The activation barriers from the lowest energy conformation of the protonated epoxides to the *trans*- and *cis*-five-membered transition structures were low (1.6−2.9 kcal/mol, HF/6-31G*), consistent with only a minor change in geometry between the reactant epoxide and the transition structures for the ring-opening process.

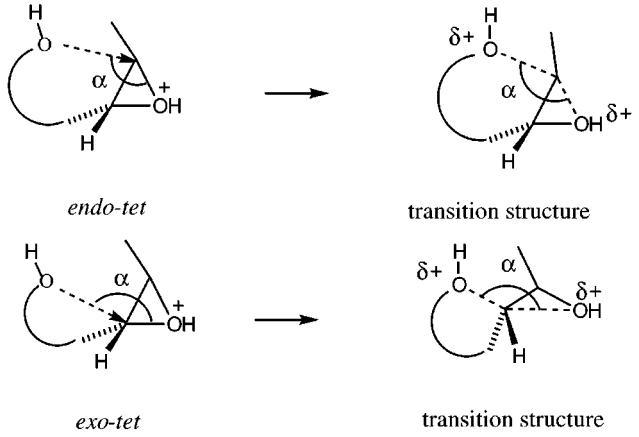

Figure 3. Schematic representation of acid-initiated epoxide ring opening in conjunction with intramolecular nucleophilic attack via *exo-tet* and *endo-tet* processes.

(9) This preference was subsequently encapsulated in the rules for ring closure enunciated by Baldwin, J. E. *J. Chem. Soc., Chem. Commun*. **1976**, *734*. See also Norman, R.; Coxon, J. M. *Principles of Organic Synthesis*; Blackie Chapman and Hall: London and John Wiley and Sons: New York, 1993; p 678. Baldwin, J. E.; Lusch, M. J. *Tetrahedron* **1982**, *19*, 2939.

(10) Ford, G. P.; Smith, C. T. *J. Am. Chem. Soc.* **1987**, *109*, 1325.

(11) Battiste, M. A.; Coxon, J. M. *The Chemistry of the Cyclopropyl Group*; Rappoport, Z., Ed.; John Wiley and Sons: New York, 1987; p 255−305.

(12) Coxon, J. M.; Morokuma, K.; Thorpe, A. J.; Whalen, D. *J. Org. Chem*. **1998**, *63*, 3875−3883.

Table 2. Energies of Minima Structures

minima structures	optimization	energy (au)	ZPFV (au)	energy + scaled ZPVE (au)[b]
		H^+		
epoxide **7** *trans*	HF/6-31G*	−384.197 51	0.202 29	−384.016 87
epoxide **10** *trans*	HF/6-31G*	−384.211 00	0.202 66	−384.030 05
		−386.598 16[a]		
furan **11** *trans*	HF/6-31G*	−384.245 21	0.205 39	−384.061 80
		−386.628 60[a]		
pyran **12** *trans*	HF/6-31G*	−384.246 64	0.206 62	−384.060 70
		−386.631 94[a]		
epoxide **15** *cis*	HF/6-31G*	−384.209 20	0.202 82	−384.028 08
		−386.597 50[a]		
furan **16** *cis*	HF/6-31G*	−384.247 54	0.205 07	−384.064 42
		−386.630 62[a]		
pyran **17** *cis*	HF/6-31G*	−384.250 00	0.206 34	−384.065 74
		−386.634 89[a]		
		BF_3		
epoxide **21** *cis*	HF/6-31G*	−707.085 87	0.206 05	−706.901 87
		−710.838 64[a]		
furan **22** *cis*	HF/6-31G*	−707.085 79	0.206 66	−706.901 25
		−710.843 96[a]		
pyran **23** *cis*	HF/6-31G*	−707.077 37	0.209 12	−706.890 63
		−710.832 46[a]		
epoxide **26** *trans*	HF/6-31G*	−707.083 33	0.205 75	−706.899 60
		−710.836 59[a]		
furan **27** *trans*	HF/6-31G*	−707.084 59	0.207 52	−706.899 28
		−710.835 83[a]		
pyran **28** *trans*	HF/6-31G*	−707.072 23	0.209 48	−706.885 17
		−710.827 75[a]		
epoxide **31** *trans*	HF/6-31G*	−707.087 25	0.206 32	−706.903 01
		−710.840 34[a]		

[a] B3LYP/6-31G* single point calculation on HF/6-31G* optimized structures. [b] ZPVE scaled by 0.961 (B3LYP) and 0.893 (HF).

Computational Methods

Exploratory calculations on the potential energy surface were carried out with the semiempirical AM1[13] model. The low energy conformations of the protonated furan and pyran products were initially determined by conformational searches at the AM1 level using the Osawa method encapsulated in Spartan.[14] All stationary points presented were obtained at the ab initio HF/6-31G* level using the GAUSSIAN 94[15] suite of programs. A selection of six-membered transition structures were optimized at the gradient-corrected hybrid density functional B3LYP/6-31G*[16] level of theory. However, difficulties were encountered locating optimized geometries for the five-membered transition structures by this method. The nature of all stationary points were confirmed through vibrational frequency analysis with transition structures characterized by the presence of one and only one imaginary frequency. Zero-point corrections (ZPC) are included in the relative energies reported with the HF/6-31G* zero point vibrational energies scaled by 0.893.

Results and Discussion

We now present ab initio molecular orbital calculations on the transition structures for inversion of configuration and related stationary points on the potential energy surface for the proton- and BF_3-assisted ring opening of *cis*- and *trans*-4,5-epoxyhexan-1-ol. For comparison, we present transition structures involving retention of configuration for protonated *cis*- and *trans*- 4,5-epoxyhexan-1-ol. The absolute and relative energies of the optimized minima and transition structures, including scaled zero point vibrational energies, are shown in Tables 1 and 2.

Houk has reported calculations at the HF/6-31G* level on the rearrangement of *trans*-4,5-epoxyhexan-1-ol with acid.[17] The epoxide was protonated on the face *cis* to the

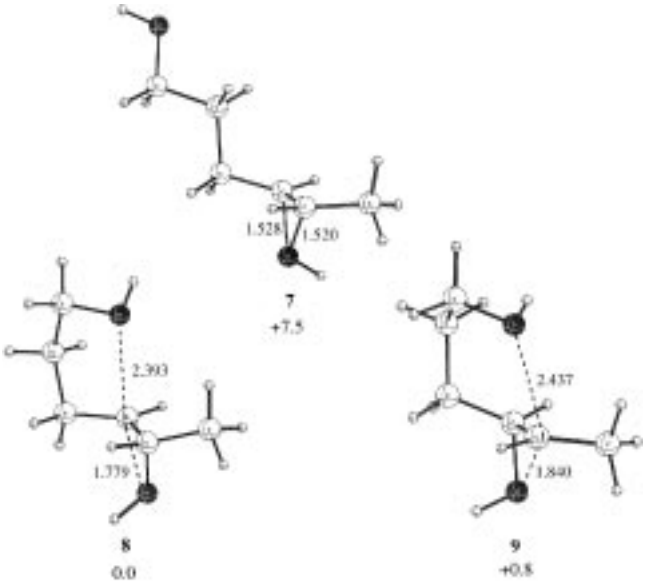

Figure 4. Transition structures **8** and **9** for ring opening of epoxide **7** as determined by Houk. The stationary points are optimized at the HF/6-31G* level, and the relative energies (kcal/mol) include zero point corrections. Bond distances are in angstroms.

(13) Dewar, M. J. S.; Zoebisch, E. G.; Healy, E. F.; Stewart, J. J. P. *J. Am. Chem. Soc.* **1985**, *107*, 3902.

(14) *SPARTAN Version 4.1*; Wavefunction, Inc.: 18401 Von Karman, Irvine, CA 92715.

(15) *Gaussian 94*, Revision D.2.; Frisch, M. J.; Trucks, G. W.; Schlegel, H. B.; Gill, P. M. W.; Johnson, B. G.; Robb, M. A.; Cheeseman, J. R.; Keith, T.; Petersson, G. A.; Montgomery, J. A.; Raghavachari, K.; Al-Laham, M. A.; Zakrzewski, V. G.; Ortiz, J. V.; Foresman, J. B.; Cioslowski, J.; Stefanov, B. B.; Nanayakkara, A.; Challacombe, M.; Peng, C. Y.; Ayala, P. Y.; Chen, W.; Wong, M. W.; Andres, J. L.; Replogle, E. S.; Gomperts, R.; Martin, R. L.; Fox, D. J.; Binkley, J. S.; Defrees, D. J.; Baker, J.; Stewart, J. P.; Head-Gordon, M.; Gonzalez, C.; Pople, J. A. Gaussian, Inc.: Pittsburgh, PA, 1995.

(16) Becke, A. D. *Phys. Rev. A* **1988**, *38*, 3098. Becke, A. D. *J. Chem. Phys.* **1993**, *98*, 1372. Lee, C.; Yang, W.; Parr, R. G. *Phys. Rev.* B **1988**, *37*, 785.

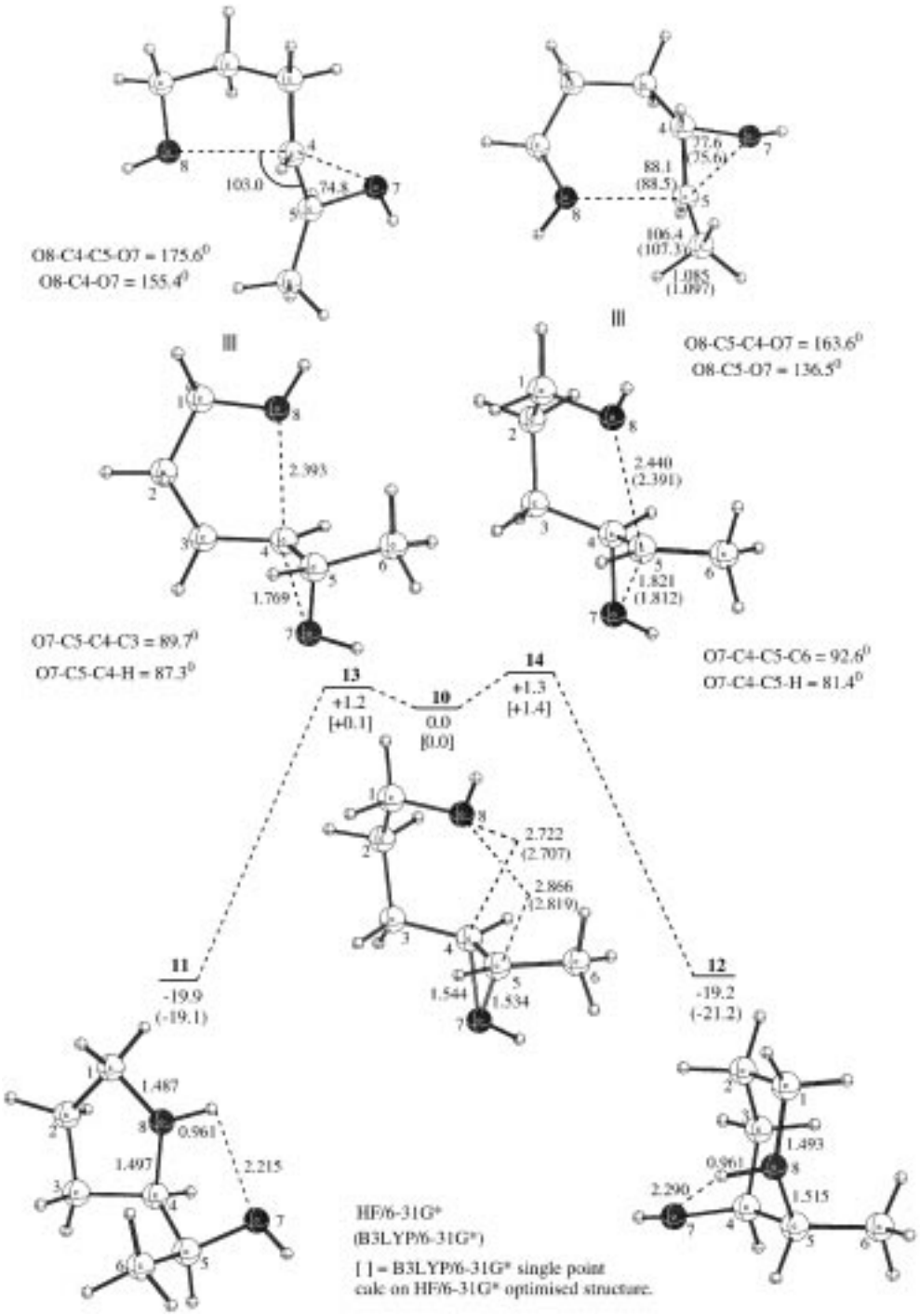

Figure 5. The potential energy surface for the rearrangement of **10** to **11** and **12**. Geometries are optimized at the HF/6-31G* level. Two perspectives of each transition structure are shown. The relative energies (kcal/mol) include zero point corrections. Bond lengths are in angstroms, and bond angles are in degrees.

hydroxyalkyl chain. The term "invertomer" has been coined[18] to describe the diastereomers resulting from positioning of the proton on either face of an epoxide. The protonated epoxide in an extended conformation **7**[19] (Figure 4) was reported[17] to be higher in energy than coiled conformers (e.g., **8** and **9**[19]). The coiled conformer, the structure of which was not given, was reported to be 10.4 and 11.3 kcal/mol lower in energy than the five- and six-membered transition structures leading to the formation of furan and pyran, respectively.

The extended conformations of protonated 3,4-epoxypentan-1-ols were also not global minima.[12] As well as seeking the global minima of protonated *trans*-4,5-epoxyhexan-1-ol, we reoptimized the extended conformation of the protonated epoxide **7**[19] at the HF/6-31G* level. Although the geometry did not change, the energy was 7.5 and 6.7 kcal/mol higher than that of transition structures **8** and **9** (Figure 4). An extended conformation of protonated epoxide **7** (though the wrong invertomer)

(17) Na, J.; Houk, K. N.; Shelvin, C. G.; Janda, K. D.; Lerner, R. A. *J. Am. Chem. Soc.* **1993**, *115*, 8453−8454.
(18) George, P.; Bock, C. W.; Glusker, J. P. *J. Phys. Chem.* **1990**, *94*, 8161−8168.
(19) We thank Professor Ken Houk an Dr. Jim Na for supplying the coordinates of their published structures.

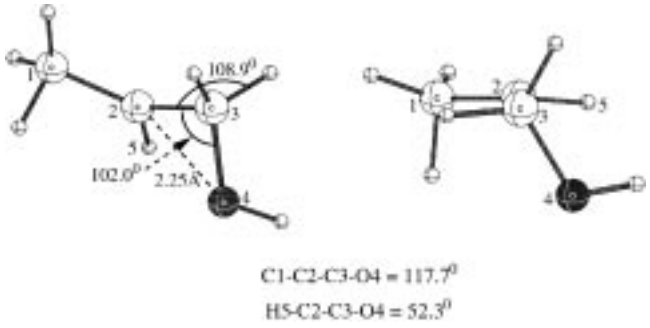

Figure 6. Two perspectives of the MP2/6-31G* optimized lowest energy transition structure for epoxide ring opening.[20]

is therefore not on the immediate reaction path to the transition structures for furan and pyran formation.

To determine the lowest energy conformations of protonated *trans*-4,5-epoxyhexan-1-ol, extensive AM1 grid search calculations involving rotation about the torsional angles of the hydroxyalkyl side chain were performed. Selected low energy conformers were optimized at the HF/6-31G* level, and the lowest energy conformer found is **10** (Figure 5). The large difference in energy between the protonated epoxide conformers **7** and **10** (8.3 kcal/mol) is an indication of the importance of charge stabilization of the C4 and C5 centers by the hydroxyl oxygen for the latter conformer. It should be noted that these are gas-phase calculations and in solution hydrogen bonding may be of lesser importance. The $C_{ep}-O$ bonds in **10** are longer than in **7**, facilitating ring opening. A schematic representation of the potential energy surface for the rearrangement of protonated *trans*-4,5-epoxyhexan-1-ol (**10**) (same invertomer as Houk) with the transition structures (invertomers of those reported by Houk) to protonated *trans*-2-methyltetrahydrofuran-3-ol **11** and protonated *trans*-2-methyltetrahydropyran-3-ol **12** is shown in Figure 5. All stationary points are fully optimized at the HF/6-31G* level.

The lowest energy conformer **10** resembles a pre-chair with the hydroxyl oxygen positioned closer to C4 (2.722 Å) than to C5 (2.866 Å). In this conformation the hydroxyl oxygen p-orbital is positioned for orbital overlap with the developing cationic center at C4 as cleavage of the C4−O7 bond occurs. The energy of **10** is close to the transition structures **13** and **14** with activation barriers of only 1.2 and 1.3 kcal/mol respectively (cf. Houk's values[17] of 10.4 and 11.3 kcal/mol).

The lowest energy conformations of the protonated furan and pyran rings **11** and **12** optimized at the HF/6-31G* level both exhibit hydrogen bonding between the hydroxyl proton and protonated ether oxygen. The rearrangement of **10** is highly exothermic and reflects the relief of epoxide ring strain. The transition structures **13** and **14** to furan and pyran are reactant-like, with a geometry closely resembling epoxide **10**.

The transition structure **13** is marginally favored (0.1 kcal/mol) over the six-membered transition structure **14**. The forming O8−C4 and breaking C4−O7 bond lengths of the former differ by less than 0.05 Å from the analogous bond lengths in **14**. The internal O8−C4−O7 bond angle (155.4°) in **13** is close to the $O-C_{ep}-O$ bond angle for the addition of water to protonated oxirane (154.9°). However for **14**, the O8−C5−O7 bond angle (136.5°) is less than optimum, reflecting poorer orbital

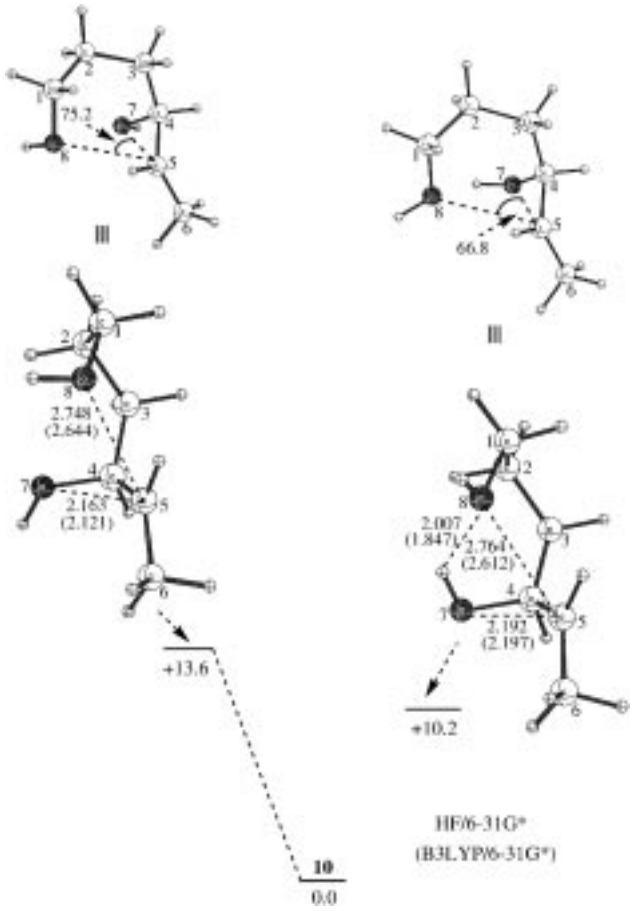

Figure 7. Six-membered transition structures involving retention of configuration for ring opening of epoxide **10** and its invertomer. Energies in kcal/mol are relative to epoxide **10**. Bond lengths are in angstroms, and bond angles are in degrees. Two perspectives of each structure are shown.

overlap and the greater strain required to form the six-membered ring.

The O8−C4−C5−O7 torsional angle (175.6°) in the forming bicyclic spiro structure **13** is close to antiperiplanar and more favorable than the analogous O8−C5−C4−O7 torsional angle (163.6°) in **14**. The latter is more constrained, reflecting bicyclic ring strain of the transition structure. It is therefore surprising that the difference in energy between **13** and **14** is as little as 0.1 kcal/mol (HF/6-31G*) favoring the former. The energy and skeletal geometry of the transition structures are almost insensitive to which face of the epoxide is protonated. The transition structure invertomers of **13** and **14** (Figure 5), namely, **8** and **9** (Figure 4), are 0.4 kcal/mol higher and 0.3 kcal/mol lower in energy, respectively. The difference in energy between the five- and six-membered transition structures **8** and **9** is 0.8 kcal/mol favoring the former, a difference moderately larger than that between **13** and **14**. We were able to fully optimize the transition structure **14** at the B3LYP/6-31G* level of theory but were unable to do so for **13**. For **14**, the optimized geometry at the HF/6-31G* and B3LPY/6-31G* levels is similar with a minor contraction in the O8−$C5^+$ (2.391 Å) and $C5^+$−O7 (1.812 Å) bond lengths observed at the latter level of theory.

Nucleophilic attack of the intramolecular hydroxy oxygen in **10** occurs in concert with the opening of the epoxide but without any substantial twisting of the

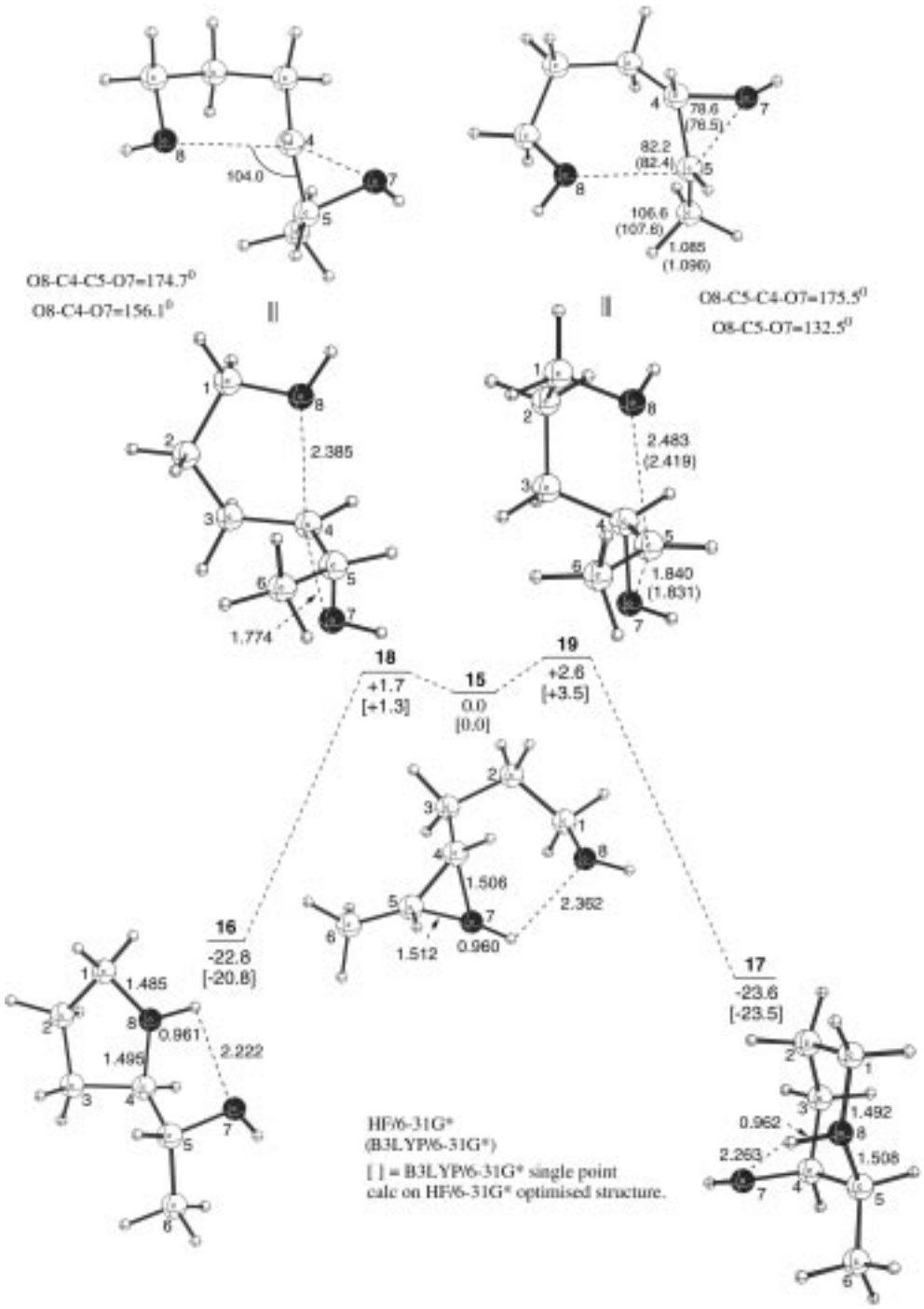

Figure 8. The potential energy surface for the rearrangement of **15** to **16** and **17** with relative energies (kcal/mol), bond distances (Å), and bond angles (degrees) at the HF/6-31G* level. Two perspectives of each transition structure are shown.

cleaving C−O bond about the epoxide C−C bond. For transition structure **13**, the O7−C5−C4−C3 and O7−C5−C4−H torsional angles are 89.7° and 87.3°, and for **14**, the corresponding O7−C4−C5−C6 and O7−C4−C5−H torsional angles are 92.6° and 81.4°, respectively. These values and the dihedrals O8−C4−C5−O7 (175.6°) for **13** and O8−C5−C4−O7 (163.6°) for **14** define the orientation of the nucleophile with respect to the epoxide plane, with the former showing a more planar interaction at the reaction center. In contrast, ring opening of protonated propene oxide occurs with substantial rotation about the epoxide C−C bond and in concert with but before hydride migration is initiated[20] (Figure 6). For this reaction, intramolecular hydride attack is late on the reaction coordinate.

Six-membered transition structures for the reaction of both **10** and its invertomer to a tetrahydropyran involving retention of configuration at the site of epoxide ring opening have been determined at the HF/6-31G* level (Figure 7). The transition structures are too high in energy for these pathways to be competitive with the reaction of the epoxide occurring with inversion of configuration. For both structures, the O8−C5−O7 bond angles (75.2° and 66.8°) reflect poor overlap of the

(20) Coxon, J. M.; Maclagan, R. G. A. R.; Rauk, A.; Thorpe, A. J.; Whalen, D. *J. Am. Chem. Soc.* **1997**, *119*, 4712−4718.

Table 3. Bond and Torsional Angles of the H^+- and BF_3-Coordinated Five- and Six-Membered Transition Structures Involving Inversion of Configuration at the Reaction Center

transition structure	bond angle		torsional angle		Δ energy (5TS − 6TS, kcal/mol)
	O8−C5−O7	O8−C4−O7	O8−C5−C4−O7	O8−C4−C5−O7	
			H^+		
13 (5TS)		155.4°		175.6°	−0.1
14 (6TS)	136.5°		163.6°		
18 (5TS)		156.1°		174.7°	−0.9
19 (6TS)	132.5°		175.5°		
			BF_3		
24 (5TS)		149.1°		175.5°	−0.3
25 (6TS)	137.1°		173.3°		
29 (5TS)		147.1°		174.4°	+0.6
30 (6TS)	141.8°		171.3°		
32 (5TS)		148.6°		177.8°	+3.4
33 (6TS)	139.3°		164.5°		

nucleophile with the epoxide bond undergoing cleavage. The transition structure from the invertomer of **10** is the lower in energy because of an intramolecular H−O8 bond (2.007 Å (HF/6-31G*) and 1.847 Å (B3LYP/6-31G*)).

Potential Energy Surface for the Rearrangement of Protonated *cis*-4,5-Epoxyhexan-1-ol (15). The potential energy surface for the rearrangement of protonated *cis*-4,5-epoxyhexan-1-ol (**15**) to protonated *cis*-2-methyltetrahydrofuran-3-ol (**16**) and protonated *cis*-2-methyltetrahydropyran-3-ol (**17**) is shown in Figure 8 for the lowest energy conformers. The rearrangement proceeds by competing pathways involving the five- and six-membered transition structures **18** and **19** with inversion of configuration at the epoxide carbons. All structures are fully optimized at the HF/6-31G* level.

The lowest energy conformation of the reactant protonated epoxide **15** is different in geometry from the isomeric protonated epoxide **10**. In the former, the hydoxyalkyl group is hydrogen bonded with the epoxide proton,[21] whereas in the latter, the hydroxyalkyl group is in close proximity to the epoxide carbons and *anti* to the epoxide oxygen. The lowest energy product conformers **16** and **17** both exhibit intramolecular hydrogen bonding between the ether proton and the hydroxyl oxygen, with the latter adopting a chair structure. The activation barriers for furan and pyran formation from **15** via transition structures **18** and **19** (1.7 and 2.6 kcal/mol) are marginally greater than the analogous barriers for the rearrangement of the *trans*-epoxide **10** (1.2 and 1.3 kcal/mol, Figure 5). The calculations show that the pathway involving a five-membered transition structure **18** leading to a furan is favored over that leading to a pyran by 0.9 kcal/mol; however, the latter product is not observed experimentally. A geometry of **19** was optimized at the B3LYP/6-31G* level that is structurally similar to the HF/6-31G* optimized geometry. The C5−O7 bond length is almost identical in both geometries (1.831 Å (B3LYP/6-31G*) and 1.840 Å (HF/6-31G*)) with only a minor reduction observed in the O8−C5 bond length (2.419 Å) in the B3LYP/6-31G* transition structure (2.483 Å (HF/6-31G*)). The transition structure **18** could not be found at the B3LYP/6-31G* level.

The O−C_{ep}−O bond and O−C_{ep}−C_{ep}−O torsional angles of the transition structures examined in this study are important parameters in defining reaction trajectory (Table 3). The O8−C4−O7 bond angle of 156.1° in transition structure **18** is close to the value for addition of water to protonated oxirane (154.9°) and comparable to the analogous angle (155.4°) for transition structure **13** for formation of furan from **10** (Figure 5). The O8−C4−C5−O7 (174.7°) and O8−C5−C4−O7 (175.7°) torsional angles for transition structures **18** and **13** are close to antiperiplanar and further reflect favorable orbital overlap for both structures. For both the reaction of **10** and **15**, transition structures **13** and **18**, respectively, represent the favored pathway and, for the latter reaction, the exclusive pathway.

For the *trans*-six-membered transition structure **14**, the O8−C5−O7 bond angle (136.5°) is more favorable and the O8−C5−C4−O7 torsional angle less favorable (163.6°) than in the *cis*-six-membered transition structure **19** (132.5°and 175.5°respectively). Because **14** is close in energy to **13** (0.1 kcal/mol), cf. **19** and **18** (0.9 kcal/mol), the more favorable O8−C5−O7 bond angle in **14** (136.5°) is the dominating feature determining the lower energy difference.

Five- and six-membered transition structures **20** and **21** for reaction with retention of configuration at the site of epoxide ring cleavage in epoxide **15** have been determined at the HF/6-31G* level (Figure 9).

The activation barriers leading to **20** and **21** from epoxide **15** are large (8.9 and 18.3 kcal/mol) in comparison with those for the pathways involving inversion of configuration for the *cis*-transition structures **18** and **19** (1.7 and 2.6 kcal/mol, Figure 8). Consequently, furan and pyran ring formation via the transition structures **20** and **21** is not expected. The retention transition structures are congested, and the epoxide C_{ep}−O7 ring opening and O8−C_{ep} ring forming bond lengths are both longer than in the inversion transition structures. The O8−C_{ep}−O7 bond angles are highly strained in both **20** (79.4°) and **21** (61.7°), and the large difference in energy between **20** and **21** favoring the former by 9.4 kcal/mol is a consequence of the lesser bicyclic ring strain in **20**. Two further transition structures for retention of configuration for the invertomer of **15** are shown in Figure 9. These are also high in energy and will not compete with the inversion pathways.

Potential Energy Surface of the Rearrangement of *cis*- and *trans*- 4,5-Epoxyhexan-1-ol with BF_3. For the BF_3-catalyzed rearrangement of the *cis*-4,5-epoxyhexan-1-ol, the potential energy surface was examined with the Lewis acid coordinated to the least hindered face *trans* to both substituents, whereas for the *trans* epoxide,

(21) The intramolecular hydrogen bond in **15** may reflect the gas-phase nature of the calculations.

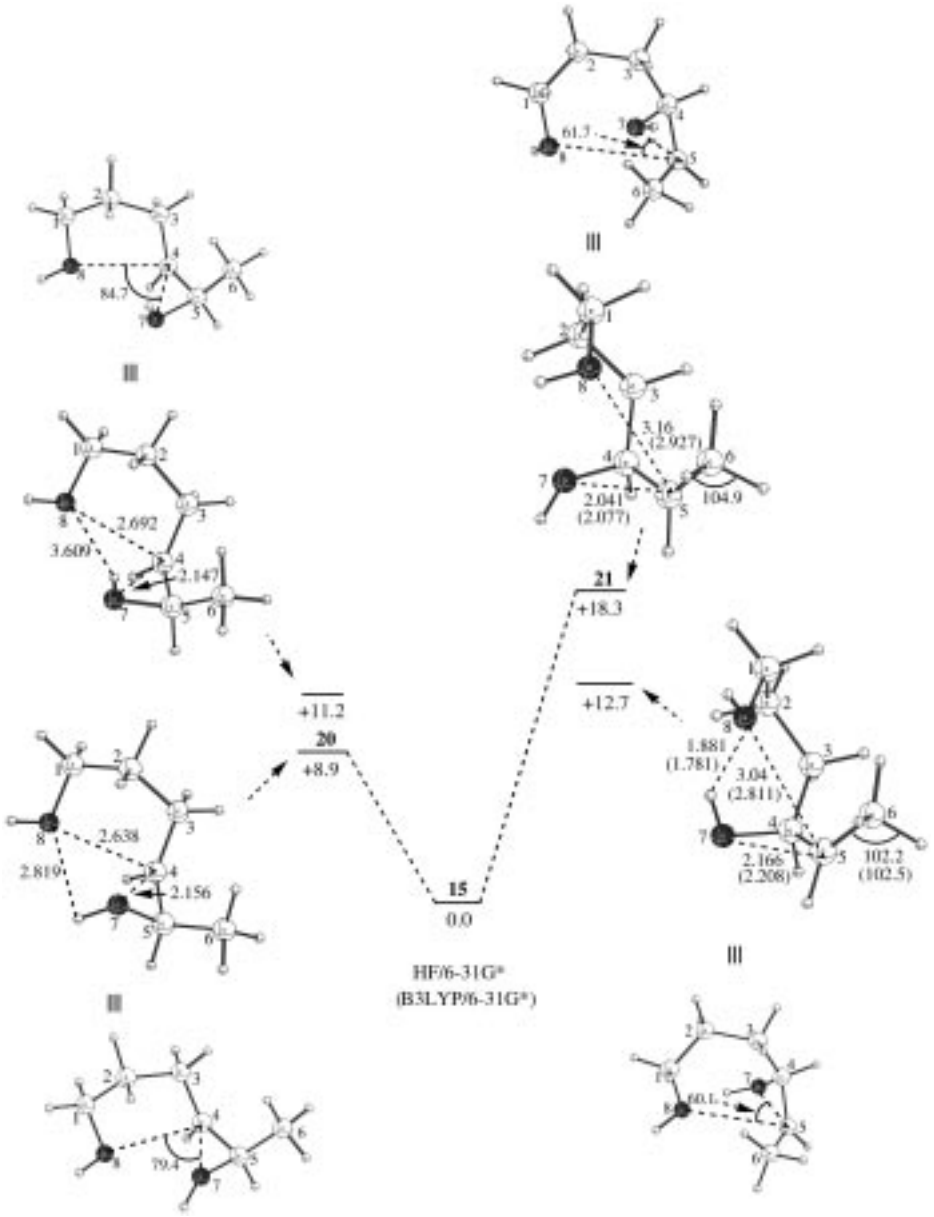

Figure 9. HF/6-31G* calculated stationary point structures (distances in angstroms, angles in degrees) for the rearrangement of **15** via transition structures **20** and **21** with retention of configuration. Also shown are the transition structure invertomers of **20** and **21**. Two perspectives of each transition structure are shown. The relative energies (kcal/mol) include zero point corrections.

the potential energy surfaces were examined with the BF_3 coordinated to each face.

(i) *cis*-4,5-Epoxyhexan-1-ol Coordinated to BF_3 *trans* to the Methyl (21). The stationary points on the potential energy surface for the rearrangement of BF_3-coordinated *cis*-4,5-epoxyhexan-1-ol **21** to the furan **22** and pyran **23** are shown in Figure 10. The activation barriers from the epoxide **21** to the five- and six-membered transition structures **24** and **25** (25.6 and 25.9 kcal/mol) are noticeably larger than the analogous activation barriers for the proton-catalyzed rearrangement (1.7 and 2.6 kcal/mol, Figure 8). The transition structures **24** and **25** are positioned near midway on the potential energy surface between the reactant epoxide **21** and the respective furan **22** and pyran **23** products and represent later transition structures in comparison with the analogous protonated transition structures **18** and **19**.

The five-membered transition structure **24** is marginally lower in energy (0.3 kcal/mol) than the six-membered transition structure **25**, with the epoxide C−O7 bonds undergoing cleavage in each being of similar length (2.072 and 2.071 Å, respectively) and significantly longer than for the protonated transition structures **13**, **14**, **18**, and **19** (1.76−1.84 Å). Intramolecular nucleophilic attack is also more advanced in both pathways than for the proton-catalysed rearrangements (2.39−2.48 Å). The bond length between the oxygen of the nucleophile and the epoxide carbon (C4−O8) is 1.908 Å in **24** and longer in **25** (O8−C5 = 2.097 Å), and because the difference between the O8−C_{ep} bond lengths in each of the furan **22** (1.476 Å) and pyran **23** (1.505 Å) products is small, **24** can be considered to be a later, more productlike transition structure than **25**. This result is in contradiction of the Hammond principle[22] because the relative energies of the products is such that **23** is 4.9 kcal/mol higher in energy than **22**. Removal of BF_3 from **22** and

(22) Hammond, G. S. *J. Am. Chem. Soc.* **1955**, *77*, 334.

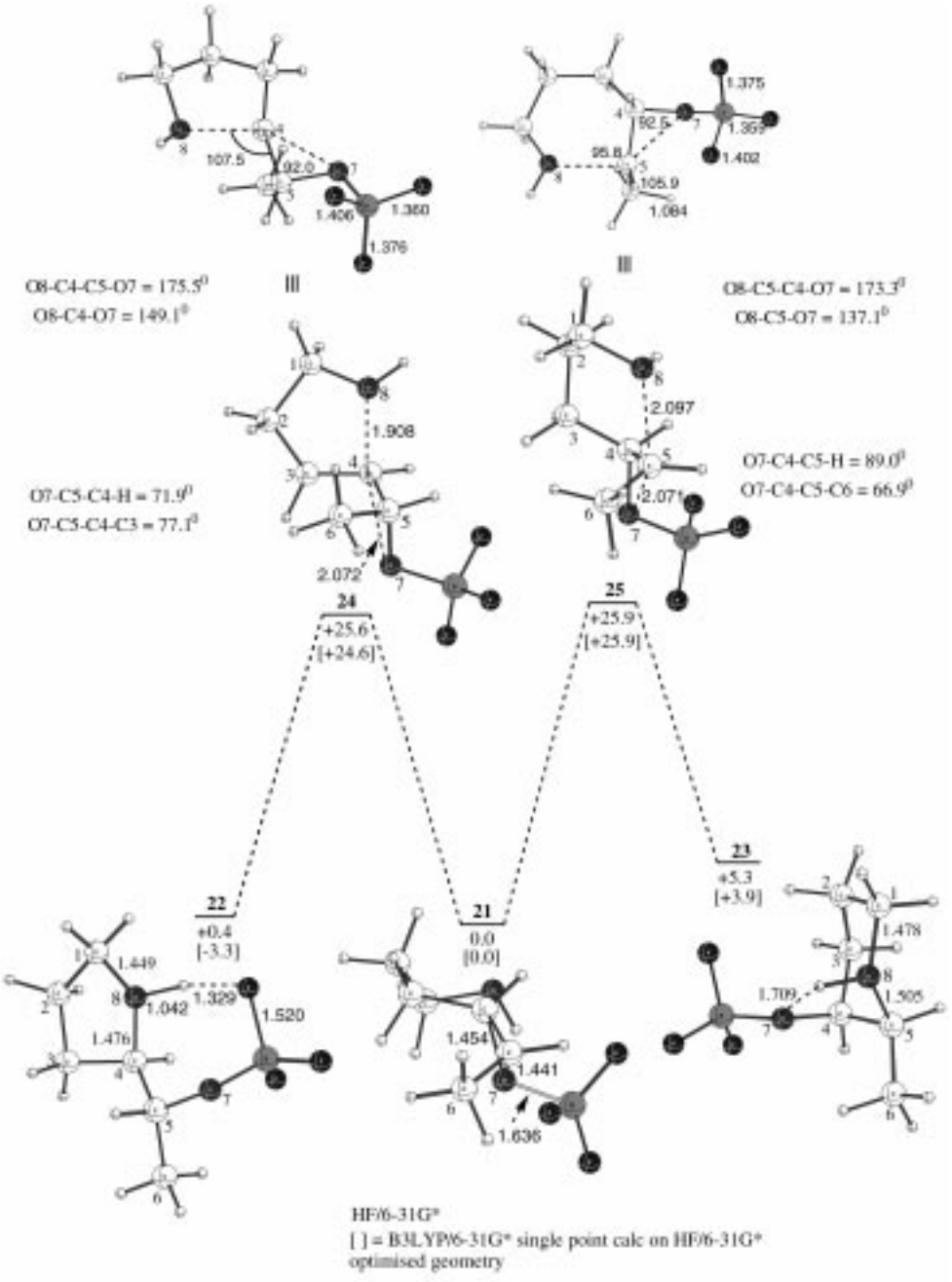

Figure 10. The potential energy surface for the rearrangement of **21** to **22** and **23**. Stationary points displayed are optimized at the HF/6-31G* level. Two perspectives of each transition structure are shown. The relative energies (kcal/mol) include zero point corrections. Bond distances are in angstroms, and bond angles are in degrees.

23 is reversible, and accordingly the uncoordinated furan and pyran products are expected to be substantially lower in energy relative to the uncoordinated epoxide, mirroring the rearrangement of the protonated epoxides **10** (Figure 5) and **15** (Figure 8).

The O8−C4−C5−O7 and O8−C5−C4−O7 torsional angles in **24** (175.5°) and **25** (173.3°) are similar, reflecting near antiperiplanar orbital overlap between the nucleophile and the epoxide. The O8−C4−O7 bond angle (149.1°) in **24** is more favorable than the corresponding O8−C5−O7 bond angle in **25** (137.1°), and the energy difference between **24** and **25** (0.3 kcal/mol) is smaller than that between the protonated transition structures **18** and **19** (0.9 kcal/mol, Figure 8) where there is a larger difference between the O8−C_{ep}−O7 bond angles (156.1° for **18** and 132.5° for **19**) (see Table 3). For the five-membered transition structure **24**, C4 is pyramidalized away from the incoming nucleophile, as evidenced by the torsional angles O7−C5−C4−H of 71.9° and O7−C5−C4−C3 of 77.1°, which reflect the lateness of the transition structure. In the same way, C5 is pyramidalized in **25** (O7−C4−C5−H (89.0°) and O7−C4−C5−C6 (66.9°)), but the transition structure is marginally less advanced along the reaction coordinate.

(ii) *trans*-4,5-Epoxyhexan-1-ol Coordinated to BF_3 *trans* to Methyl (26). For *trans*-4,5-epoxyhexan-1-ol, both faces of the epoxide can be coordinated with BF_3, and stationary points on the potential energy surface for reaction of both invertomers are examined. The station-

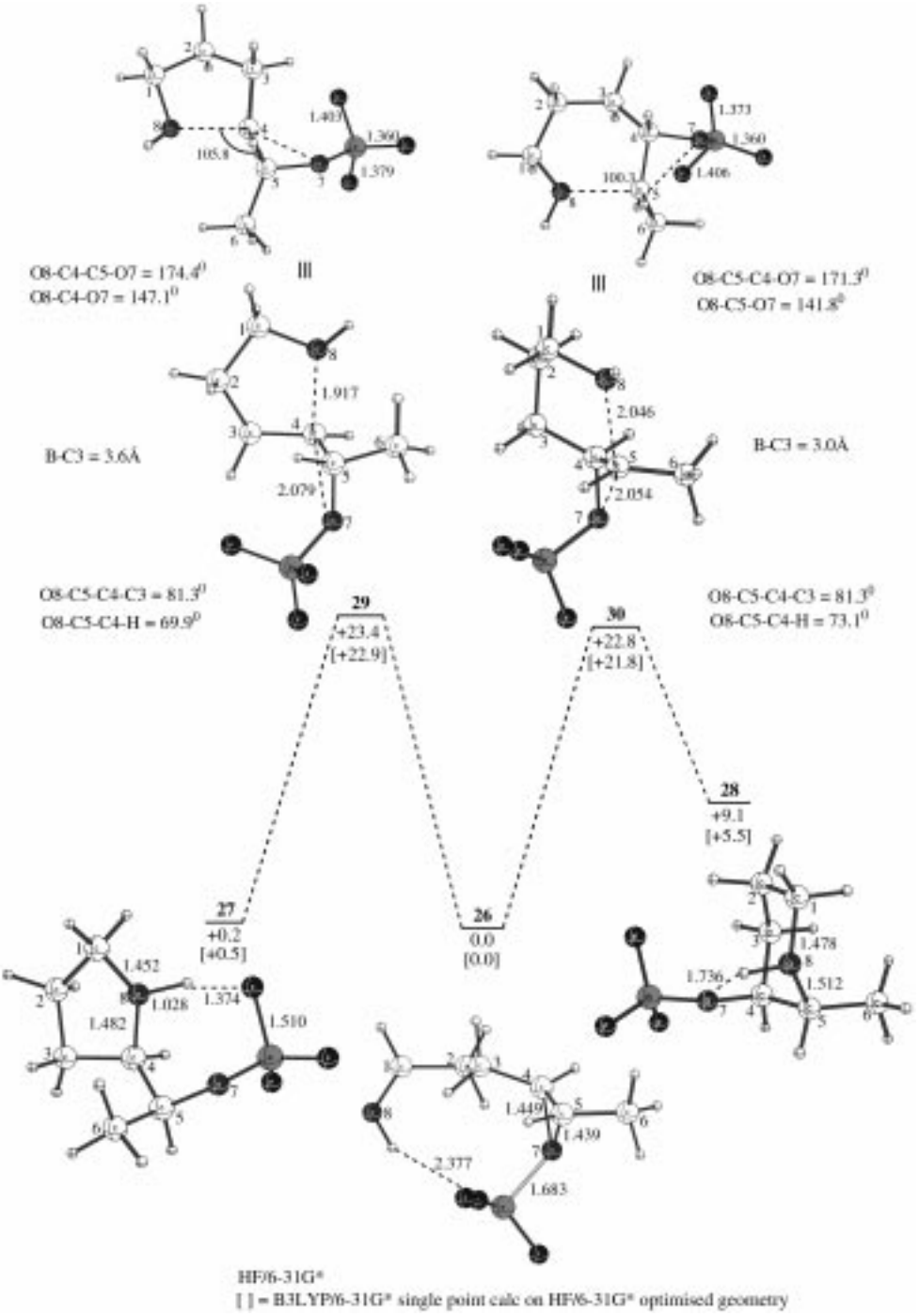

Figure 11. The potential energy surface for the rearrangement of **26** to **27** and **28** optimized at the HF/6-31G* level. The relative energies (kcal/mol) include zero point corrections. Two perspectives of each transition structure are shown, with bond lengths in angstroms, and bond angles in degrees.

ary points on the potential energy surface for the rearrangement of *trans*-4,5-epoxyhexan-1-ol with BF_3 coordinated to the epoxide *cis* to the hydroxyalkyl chain (**26**), which is the lower energy invertomer (by 2.1 kcal/mol), are shown in Figure 11.

Calculations at the HF/6-31G* level show that ring opening at the C4 position and nucleophilic attack of the hydroxyl to give the five-membered transition structure **29** is less favored (by 0.6 kcal/mol) over nucleophilic attack at C5 to give pyran by way of transition structure **30**. This result contrasts to the proton-catalyzed rearrangement of *trans*-4,5-epoxyhexan-1-ol **10** (Figure 5) in which the pathway involving a five-membered transition structure is favored over pyran formation. The experimental results with BF_3 as catalyst show a furan to pyran ratio of 84:16. It is somewhat surprising that **30** is calculated to be lower in energy than **29** given that the BF_3 group in the former is in closer proximity with the hydroxyalkyl side chain (B−C3 = 3.0 Å) than in **29** (B−C3 = 3.6 Å), while in the latter, the BF_3 is nearly eclipsed with the C5−H (B−O7−C5−H = 7.9°).

The potential energy surfaces in Figures 5, 8, and 10 have shown that the energy difference between the five- and six-membered transition structures decreases as the O8−C5−O7 bond angle of the six-membered transition structure becomes closer to the O8−C4−O7 bond angle

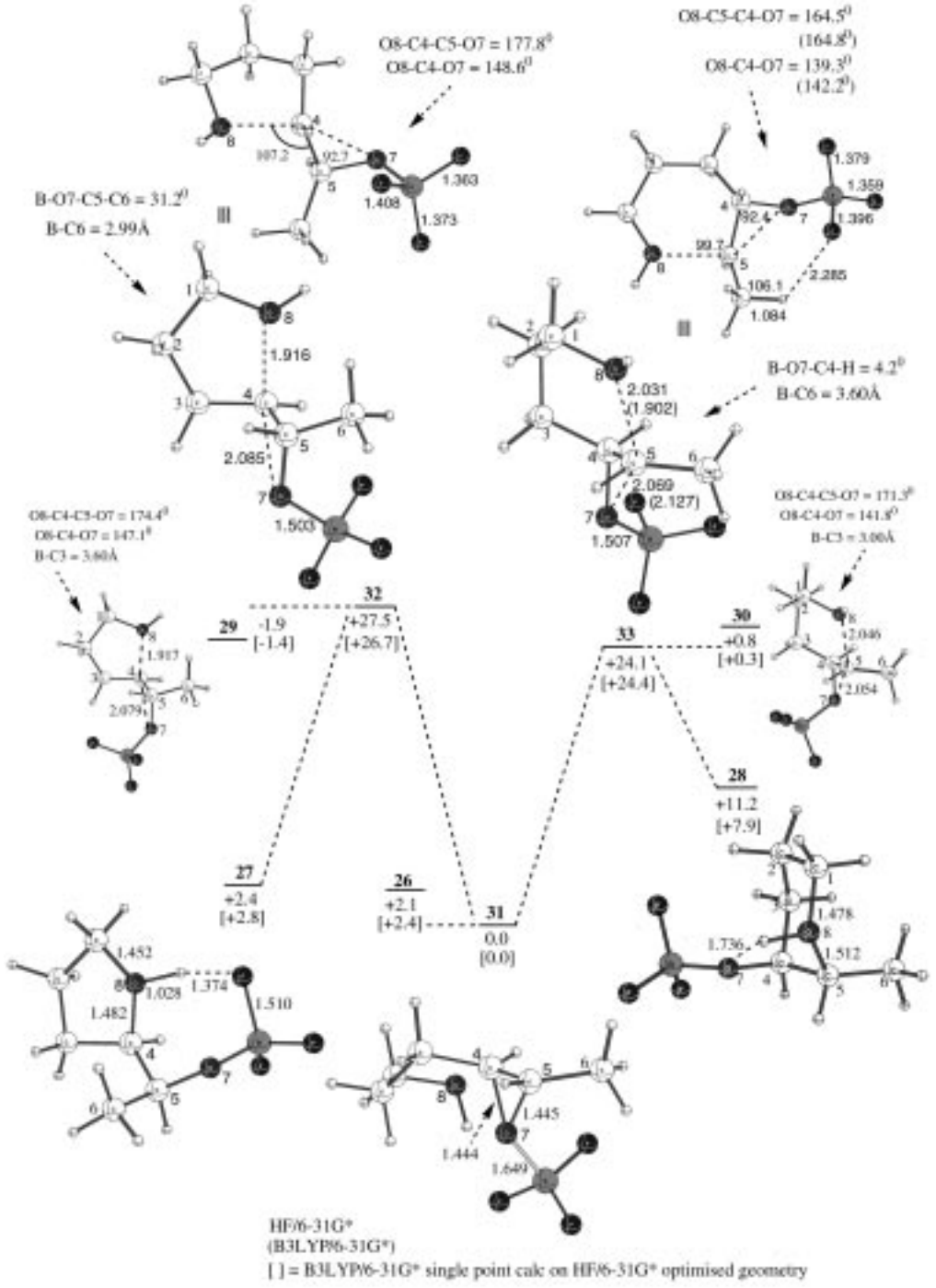

Figure 12. The potential energy surface for the rearrangment of **31** to **27** and **28**. Structures presented are optimized at the HF/6-31G* level. Two perspectives of the transition structures **32** and **33** are shown. The relative energies (kcal/mol) include zero point corrections. Bond lengths are in angstroms, and bond angles are in degrees.

of the five-membered transition structure (see Table 3). The O8−C5−O7 bond angle of **30** (141.8°) is more favorable than the corresponding bond angle in the six-membered transition structures **14** (136.5°), **19** (132.5°), and **25** (137.1°) and is only 5.3° smaller than the O8−C4−O7 bond angle in **29** (147.1°). The ring forming and ring opening bond lengths of the *trans*- five- and six-membered transition structures **29** and **30** are similar to the corresponding bond lengths in the *cis*- five- and six-membered transition structures **24** and **25** (Figure 10). The only notable difference is the moderately tighter O8−C5 (2.046 Å) and C5−O7 (2.054 Å) bond lengths in **30** in comparison to **25** (O8−C5 = 2.097 Å and C5−O7 = 2.071 Å).

Transition structure **29** can be considered to be more productlike in geometry than transition structure **30** by comparison of the O8−C_{ep} bond lengths in each relative to the O8−C_{ep} bond lengths in the respective furan **27** and pyran **28** products. The difference between the O8−C4 bond lengths in **29** (1.917 Å) and in furan **27** (1.482 Å) is 0.435 Å, moderately smaller than the difference between the O8−C5 bond lengths in **30** (2.046 Å) and in

pyran **28** (1.512 Å) of 0.534 Å. For the five-membered transition structure **29**, C4 is pyramidalized away from the incoming nucleophile, as evidenced by the torsional angles O7−C5−C4−H of 69.9° and O7−C5−C4−C3 of 81.3°, reflecting the lateness of the transition structure. In the same way, C5 is similarly pyramidalized in **30** (O7−C4−C5−H (73.1) and O7−C4−C5−C6 (81.3)), but the transition structure is marginally less advanced along the reaction coordinate.

(iii) *trans*-4,5-Epoxyhexan-1-ol Coordinated to BF_3 *cis* to Methyl (31). The optimized stationary points on the HF/6-31G* potential energy surface for the rearrangement of **31** to furan **27** and pyran **28** are displayed in Figure 12. The transition structures **29** and **30** for the rearrangement of the invertomer **26** are included on the potential energy surface for comparison. Intramolecular nucleophilic attack and epoxide ring opening at C4 in **31**, leading to transition structure **32**, is 3.4 kcal/mol higher in energy than the pathway via transition structure **33** leading to pyran formation. This result is in contrast to the experimental results, where furan is preferentially formed. The BF_3 group is eclipsed with an adjacent proton (B−O7−C4−H = 4.2°, B−C4H = 3.6 Å) in **33** and is in a sterically less crowded position than in **32**, in which the BF_3 group is close to the methyl (B−O7−C5−C6 = 31.2°, B−C6 = 2.99 Å).

The ring forming and ring breaking bond lengths in **33** (O8−C5 (2.031 Å) and C5−O7 (2.069 Å)) and **32** (O8−C4 (1.916 Å) and C4−O7 (2.085 Å)) are similar to the corresponding bond lengths of the five- and six-membered transition structures **29** and **30** (Figure 11) and are more advanced than the proton-catalyzed transition structures. A B3LYP/6-31G* optimized geometry of **33** was determined and shown to have O8−C5−O7 bond and O8−C5−C4−O7 torsional angles (142.2° and 164.8°, respectively) similar to the analogous angles in the HF/6-31G* optimized geometry (139.3° and 164.5°). Intramolecular nucleophilic attack and epoxide ring opening is more advanced in the B3LYP/6-31G* optimized geometry of **33**, as defined by the O8−C5 (1.902 Å) and C5−O7 (2.127 Å) bond lengths. An optimized geometry of **32** at the B3LYP/6-31G* level was not found.

The O8−C4−O7 bond angle (148.6°) and the O8−C4−C5−O7 torsional angle (177.8°) in **32** show that more favorable orbital overlap is achieved at the reaction center than in transition structure **33** (O8−C5−O7 (139.3°) and O8−C5−C4−O7 (164.5°)). Intramolecular nucleophilic attack is more advanced in the former, as evidenced by the shorter O8−C4 (1.916 Å) bond length in comparison with the O8−C5 bond length in **33** (2.031 Å) relative to the O8−C_{ep} bond lengths in the furan **27** (1.482 Å) and pyran **28** (1.512 Å) products. The difference in energy between the five-membered transition structures **29** and **32** favoring the former by 1.9 kcal/mol is attributed to the sterically less crowded position of the BF_3 group in **29** (B−C3 = 3.60 Å) compared with that in **32** (B−C6 = 2.99 Å). Both structures show favorable orbital overlap at the C4 reaction center with little variation observed between the O8−C4−O7 bond and O8−C4−C5−O7 torsional angles for each (see Figure 12). The positioning of the BF_3 group in the six-membered transition structures **33** and **30** is also an important geometrical feature affecting the relative energy of each. Transition structure **33** is 0.8 kcal/mol lower in energy than transition structure **30** as a result of the more favored position of the BF_3 group in the former (B−C6 = 3.60 Å) compared with that in the latter (B−C3 = 3.0 Å). The smaller energy difference between **33** and **30** (0.8 kcal/mol) compared with the energy difference between **29** and **32** (1.9 kcal/mol) is most likely due to the poorer orbital overlap associated with transition structure **33** (O8−C4−O7 (139.3°) and O8−C5−C4−O7 (164.5°)) compare with that in **30** (O8−C5−O7 (141.8°) and O8−C5−C4−O7 (171.3°)).

The BF_3-coordinated *cis*- and *trans*- five-membered transition structures **24**, **29**, and **32** show similar values for the O8−C4−O7 bond angles (see Table 3), which are 6−9° less than in the *cis*- and *trans*-protonated five-membered transition structures **13** and **18**. The O8−C4−C5−O7 torsional angles for **24**, **29**, and **32** are comparable to those for **13** and **18** and are close to ideal for maximum orbital overlap. For the BF_3-coordinated six-membered transition structures **25**, **30**, and **33**, the O8−C5−O7 bond angles are more favorable than for the protonated transition structures **14** and **19** and reflect a more advanced degree of bond formation at the transition structure. The O8−C_{ep}−C_{ep}−O7 torsional angles for all of the six-membered transition structures examined in this study vary somewhat, with the torsional angles for the *trans*-six-membered transition structures **14** (163.6°) and **33** (164.5°) poorer than those in the *cis*-six-membered transition structures **19** (175.5°) and **25** (173.3°).

Conclusion

For rearrangement of protonated *cis*- and *trans*-4,5-epoxyhexan-1-ol, the pathway involving a five-membered transition structure in each case is marginally favored over pyran formation. The energy difference between the five- and six-membered transition structures is more sensitive to change in the O−C_{ep}−O bond angle than in the O−C_{ep}−C_{ep}−O torsional angle. The transition structures are reactant-like, with minimal epoxide ring opening at the transition structure. The transition structures for furan and pyran formation for the BF_3-catalyzed rearrangement of *cis*- and *trans*-4,5-epoxyhexan-1-ol are more advanced than those for the corresponding protonated transition structures. The main structural variation between the five- and six-membered transition structures is the extent of intramolecular nucleophilic attack, which is more advanced in the five-membered transition structures. For the BF_3-catalyzed rearrangement of *cis*-4,5-epoxyhexan-1-ol, the calculations show a pathway involving a five-membered transition structure is favored and is in agreement with the experimental result where furan is formed exclusively. The potential energy surface for rearrangement of each invertomer of protonated *trans*-4,5-epoxyhexan-1-ol is in contrast to the experimental results and favors pyran formation in preference to furan.

Acknowledgment. We acknowledge grants from the New Zealand Lotteries Board and New Zealand Government Marsden Fund.

Supporting Information Available: Archive material on all stationary points. This material is available free of charge via the Internet at http://pubs.acs.org.

JO990364D